INNOVATIVE MECHANICAL ENGINEERING **ISSN 2812-9229 (Online)**
University of Niš, Faculty of Mechanical Engineering
VOL.4, NO 1, 2025, PP. 59-84

Original scientific paper *

INTERPRETING INTEGRATION CONSTANTS IN ELASTIC BEAM THEORY

Julijana Simonović[1], Marija Stamenković Atanasov[1] and Dragan B. Jovanović[1]

[1]Faculty of Mechanical Engineering University of Niš, Serbia

Abstract. *The linear elastic theory of bending is used to derive the differential equation of the elastic curve of a bent beam. Solving this second-order differential equation requires two integration constants for each beam section between supports. The direct integration method, together with the Clebsch procedure, is used to obtain the elastic curve equation. This paper explains the physical meaning of these integration constants. Various loading positions and scenarios are considered for several overhanging elastic beams, and the shape of the elastic curve is presented for each case. The beam bending stiffness is kept of a constant value for a given cross-section and material of the beam, and we show its correlation with the integration constants. We apply the criterion of the ultimate bending strength (flexural strength) of steel for dimensioning beams. Thus, the characteristic dimension of the profile is determined according to the maximum value of the bending moment for each type of beam, considering the values and distribution of the load. In this context, the selected examples have the same cross-section profiles but different stiffnesses, as each is dimensioned individually according to the changing loading values and distribution. We also consider overhanging beams, and how the deflection orientation correlates with the integration constants, which depend on the position and magnitude of the load. Our findings show that even slight changes in the magnitude of concentrated forces can significantly affect deflection behaviour. This effect, referred to as "dog's tail movement," was especially noticeable at the free ends of overhanging beams. This underscores the crucial need for precise determination of load factors in practical applications.*

Key words: *Overhanging elastic beam, Dog's tail movement, Direct integration method, Clebsch procedure, Integration constants, Bending stiffness.*

*__Received: March 20, 2025 / Accepted April 16, 2025.__
Corresponding author: Julijana Simonović
Faculty of Mechanical Engineering University of Niš, Serbia
E-mail: julijana.simonovic@masfak.ni.ac.rs

1. INTRODUCTION

In contemporary engineering practices, understanding the elastic properties of materials is crucial. This paper focuses on interpreting integration constants within the framework of linear bending theory, examining their physical significance in explaining beam deformations under various loads. The objective of this research is to introduce new foundations for the efficient design and analysis of structural bent elements by analysing integration constants and their correlation with deflection orientation and bending stiffness.

We begin this paper by applying the linear theory of stress and strain in pure bending to derive the equation of the elastic curve. The resulting equation is a nonlinear second-order differential equation, with its integral being elliptic. Thus, we use a linearized approximation to solve the differential equation of the elastic curve. It was found that the deviation of the deflection results obtained by the approximate differential equation was up to 4% compared to the results obtained by the exact differential equation, and in extreme cases, the deviation was up to a maximum of 10%, [1]. The study [1] demonstrated a robust numerical method that effectively addresses the complexities of beam behaviour, particularly when dealing with variable cross-sections. The authors address the boundary value problem by transforming it into an initial value problem using a special application of the shooting method. This transformation allows for high accuracy in obtaining the initial values of the differential equations. The authors also compared their numerical results with analytical solutions and finite element method (FEM) results. This comparison demonstrates a good agreement of all obtained results. This provides a strong foundation for using modern numerical methods to derive solutions for complex loading scenarios.

With the advent of advanced numerical methods, the elliptic integral can be solved, allowing the exact solution to be determined if necessary. Approximate numerical methods, such as the finite element method (FEM) or finite difference method (FDM), simplify the problem by discretizing the beam into smaller segments or elements [2]. These methods are computationally efficient and can handle complex geometries and loading conditions more easily than exact solutions. Approximate solutions can be iteratively improved by refining the mesh or increasing the number of segments, thus approaching the exact solution.

The application of the theory of pure bending shows that the influence of shear forces can be neglected. However, in the case of general bending by forces, this influence is not negligible. The importance of references such as [3, 4] is highlighted, as their work provides mathematical models of elastic curves for simply supported beams subjected to uniformly distributed and concentrated loads, considering shear effects. In [3], Rojas presents a model that demonstrates how shear deformations affect the elastic curve of the beam, which is crucial for accurately predicting deformations in beams made of composite or metamaterials. The study emphasizes that traditional models that neglect shear deformations are not sufficiently accurate for modern materials and structures. In [4], Rojas and Espino focus on calculating fixed-end moments for beams subjected to a concentrated force localized anywhere along the beam, considering shear deformations. Their study shows that including shear deformations significantly alters the values of fixed-end moments, allowing for more precise engineering calculations and better assessment of beam behaviour under various loading conditions. Their research underscores the importance of including these effects for more accurate and realistic modelling of beam behaviour under various loading conditions.

The exact solution of the elastic curve can be mathematically complex, especially for beams with irregular shapes, varying material properties, especially with discontinuities, or complex boundary or loading conditions. Nevertheless, contemporary research suggests generalized solutions for beams with discontinuities on elastic foundations [5]. While it is possible to find exact solutions for complex scenarios, the fundamental understanding of the elastic curve concept is often lacking when interpreting these solutions.

In engineering practice, it is crucial to comprehend the solutions generated by software that uses approximate methods. Our approach aims to connect practical engineering solutions with the underlying meaning of the results. Achieving this requires a solid physical understanding of all the terms in the mathematical models and their solutions, including how integration constants relate to deflections and bending stiffness. The latter represents a central theme explored throughout this work.

Through this investigation, we aim to enhance the design and analysis of structural elements by clarifying the interplay between mechanical loads and beam behaviour, leading to better-based engineering decisions and safer structures.

In this paper, we delve deeper into bent beams and their structural integrity, focusing particularly on the physical meaning of integration constants in the bending theory of elastic beams. Following our initial exploration, the subsequent sections systematically address various facets of this topic.

Section 2 introduces the concepts of stress and strain in pure bending. It establishes the relationship between applied loads, moments, and the corresponding stress distributions, providing a theoretical framework for understanding the behavior of beams under load.

Section 3 presents the differential equation governing the elastic curve of a bent beam. This is crucial for calculating deflections and understanding the bending moment's role in beam analysis. The section discusses methods of deriving the elastic curve, emphasizing the importance of both integration constants and the material's bending rigidity.

Section 4 elaborates on the Clebsch procedure, a significant method for calculating beam deflection under various loading conditions. This section outlines a systematic approach to integrate piecewise functions to derive bending moments and deflections across the entire span of a beam.

Section 5 focuses on numerical results and discussions, showcasing overhanging beam studies with varying loads and heights of cross-sections. Here, we analyze how the integration constants correlate with beam deflection and the nuances of their behavior under different loading scenarios.

Finally, in the Conclusion, we synthesize our findings, summarizing the significance of integration constants in practical engineering contexts and suggesting directions for further research. Ultimately, this work aims to enhance the design and analysis of structural elements by clarifying the interplay between mechanical loads and beam behavior.

From the results of this study, engineers can gain better insights into the behavior of bent beams under various types, sizes, and arrangements of loads, which will help them design structures more effectively and select appropriate profiles for given material characteristics.

2. STRESSES AND STRAINS IN PURE BENDING

Let us consider a beam, as shown in Fig.1, with two equal overhangs each of length c, loaded at the free ends with forces F. The section of the beam between supports A and B is subjected to moments $M = F \cdot c$, acting in the vertical plane of the load through the longitudinal axis Az of the beam. In the cross-sections between supports A and B, there are no transverse (shear) forces, as seen in the F_T diagram of Fig. 1a, and the bending moment has a constant value $M = F \cdot c$, as shown in the M_f diagram in Fig. 1a. Under the influence of these moments, the beam in the span AB deforms such that the upper fibers elongate, and the lower fibers shorten, as seen in Fig. 1b. The elongations are greater for fibres closer to the upper edge $a - a$ compared to fibres $b - b$ which are further from the edge. Conversely, fibres $d - d$ on the lower outer edge will shorten the most (more than fibres $c - c$, Fig. 1b). Between the fibres that elongate and the fibres that shorten lie the fibres that do not change in length. These fibres are called neutral fibres ($0 - 0$), and they form the neutral surface, whose intersection with the bending plane R_s is the neutral axis (line) or the elastic curve of the beam. The neutral axis within the beam experiences no strain and stress, while they increase linearly from it. It divides the beam into two regions: one under compression and the other under tension.

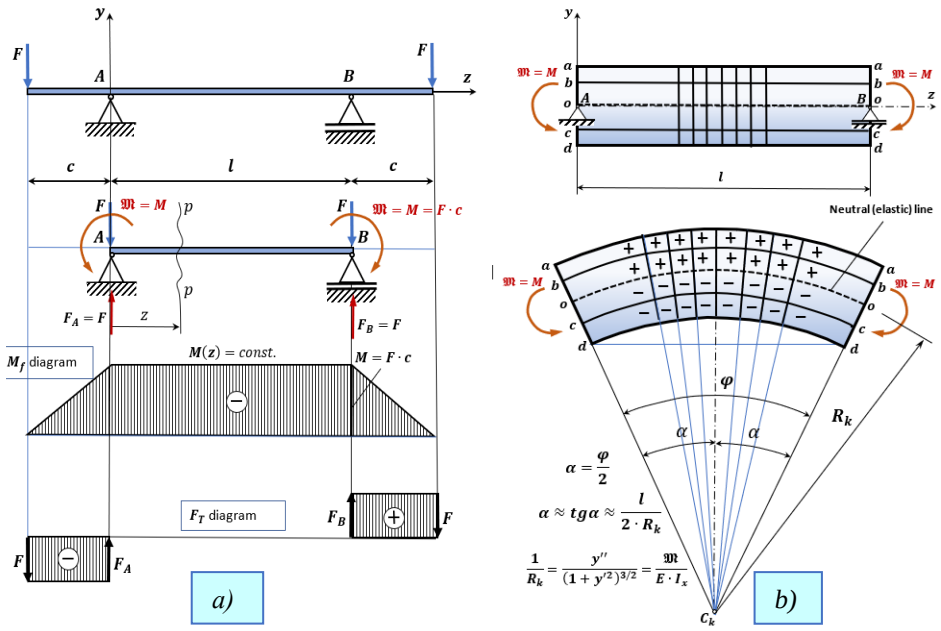

Fig. 1 Pure bending: a) example of loading and b) deformations, neutral axis $0 - 0$, a-a and b-b stretched and extended fibres, c-c and d-d compressed and shortened fibres, [7].

When the direction of the moments is reversed, the deformation of the beam is also reversed. In this case, the top fibres of the beam experience compressive stress and thus shorten, while the bottom fibres experience tensile stress and elongate, as shown in Fig. 2.

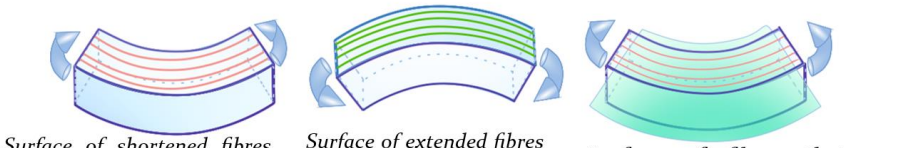

Surface of shortened fibres that are compressed (d-d and c-c in Fig. 1 b)

Surface of extended fibres that are streched (a-a and b-b in Fig. 1 b)

Surface of fibres that are without deformations -neutral surface (o-o in Fig. 1 b)

Fig. 1 Bending deformation surfaces, [7].

This type of stress, caused by moments acting in the plane of the load that coincides with the centroidal plane, where the only load throughout the span is the constant bending moment $M_f = const.$ without the transverse force, $F_T = 0$, is known as pure bending. The theory of pure bending assumes that the material is homogeneous and isotropic, and that the beam is initially straight and remains plane after bending. In reality, a state of pure bending does not practically exist, because such a state needs an absolutely weightless member. The state of pure bending is an approximation made to derive formulas.

To establish the relationship between fibre deformation and the stress resulting from external moment loads, we consider two closely spaced cross-sections at a distance dz, as shown in Fig.3 a). Under the action of moments $M = F \cdot c$, the cross-sections rotate relative to each other by an angle $d\varphi$, but it is assumed that their surfaces remain flat as before deformation (Bernoulli's hypothesis). The neutral line intersects the cross-sections at points O and O', with the distance between them remaining unchanged $\overline{OO'} = dz$.

If we observe the fibres above the neutral line, we see that they elongate. For example, the distance between points B and B', which belong to fiber $b - b$ at a distance y from the neutral line, changes by an elongation $\overline{B''B'} = \Delta dz$, so the strain of that fibre is $\varepsilon_z = \Delta dz/dz$.

According to Hooke's law, this strain corresponds to a normal stress $\sigma_z = E \cdot \varepsilon_z$, which acts at point B in the axial direction perpendicular to the cross-section OB. From Fig. 3a, based on the similarity of the arc triangles (for small angles $d\varphi \to 0$, it is assumed that the arc can be approximated by a straight line) $\Delta C_k OO' \sim \Delta O'B'B''$, the relationship can be written as:

$$\frac{\Delta dz}{dz} = \frac{y}{R_k} = \varepsilon_z = \frac{\sigma_z}{E}, \tag{1}$$

where R_k is the radius of curvature of the elastic curve. The elastic curve is a curved line with the centre of curvature C_k. In the points of the cross-section, normal stresses occur that are proportional to the distance y of the fibres from the neutral axis (neutral surface):

$$\sigma_z = \frac{E}{R_k} y. \tag{2}$$

To determine the relationship between the normal stress and the bending moment M_f, the equilibrium of the beam section to the left of the cross-section $p - p$ is considered, as shown in Fig.3 b). The effect of the beam section to the right of the cross-section $p - p$ is replaced by internal forces, which are reduced to the moment couple $\overrightarrow{\mathfrak{M}} = \vec{M}(z)$ in the opposite direction. On the elementary surface dA of the cross-section, elementary force

$dZ = \sigma_z dA$ act perpendicular to the cross-section. Based on the previous and Fig. 3b, six equilibrium conditions for the observed cross-section can be written as:

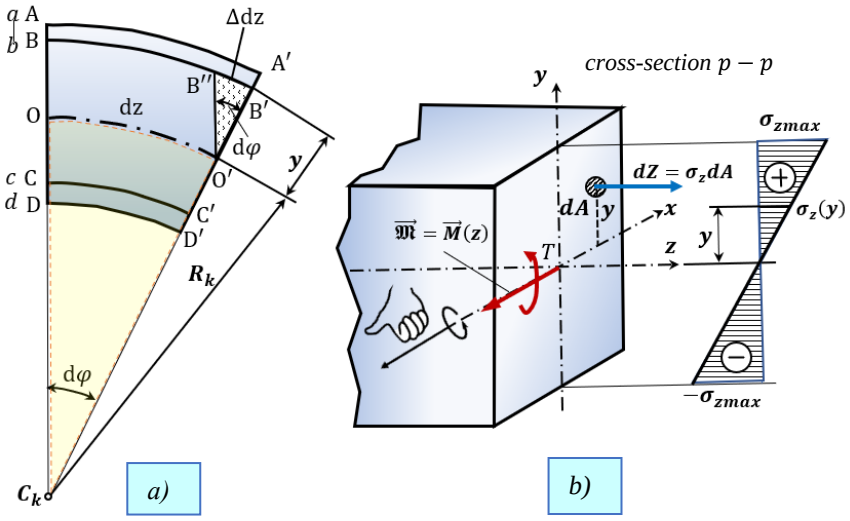

Fig. 2 a) The segment of the bent beam between two cross-sections that are relatively rotated by a small angle $d\varphi$; b) Reaction force dZ at small area dA of the cross-section and normal stress distribution over the cross-section, [7].

$$1)\ \sum X_i \equiv 0, \qquad 2)\ \sum Y_i \equiv 0,$$

$$3)\ \sum Z_i = \int_A \sigma_z\, dA = 0,$$

$$4)\ \sum M_x = 0,\ \text{thus:}\ -M(z) + \int_A y \cdot \sigma_z \cdot dA = 0,$$

$$5)\ \sum M_y = 0,\ \text{thus:}\ -\int_A x \cdot \sigma_z \cdot dA = 0,$$

$$6)\ \sum M_z \equiv 0.$$

Conditions 1, 2, and 6 are identically satisfied, and from the equilibrium condition given by expression 3 and Eq. (2), it follows:

$$\int_A \frac{E}{R_k} y \cdot dA = \frac{E}{R_k} \int_A y \cdot dA = \frac{E}{R_k} S_x = 0,$$

from which it follows that the first moment of area in the x direction must be zero $S_x = 0$, which is satisfied only if the x-axis is the centroidal axis. Since for all points on this axis $y = 0$, according to Eq. (2) it follows that $\sigma_z = 0$. The x-axis is therefore the neutral axis, which is the geometric locus of points in the cross-section where the normal stress is zero.

From condition 4 it follows:

$$M(z) = \int_A y \cdot \sigma_z \cdot dA = \int_A y \cdot \frac{E}{R_k} \cdot y \cdot dA = \frac{E}{R_k} \int_A y^2 \cdot dA = \frac{E}{R_k} I_x \, .$$

If we introduce the relation $\frac{\sigma_z}{y} = \frac{E}{R_k}$, which follows from Eq. (2), then the relation between bending moment and normal stress in cross-section is:

$$M(z) = \frac{\sigma_z}{y} I_x \, ,$$

so that the expresion for normal stress depending on bending moment is as follows:

$$\sigma_z = \frac{M(z)}{I_x} y \, . \tag{3}$$

It can be observed that the normal stress is a linear function of the coordinate y for the given cross-section, and its maximum value occurs in the edge fibers of the section, i.e., at $y = y_{max}$, as illustrated in the diagram in Fig. 3b.

From condition 5 and Eq. (2) follows that:

$$\int_A x \cdot \frac{E}{R_k} \cdot y \cdot dA = \frac{E}{R_k} \int_A x \cdot y \cdot dA = \frac{E}{R_k} I_{xy} = 0 \, .$$

This condition is satisfied only if the centrifugal moment of inertia for the observed centroidal axes is zero ($I_{xy} = 0$), which holds true when at least one of the axes (x and/or y) is a principal centroidal axis.

From Eqs. (2) and (3), a formula for the radius of curvature of the elastic curve can be derived:

$$\frac{1}{R_k} = \frac{M(z)}{E \cdot I_x} = \frac{M(z)}{\mathfrak{B}_x} , \tag{4}$$

where $\mathfrak{B}_x = E \cdot I_x$ is the bending stiffness (flexural rigidity), with dimensions $[F \cdot L^2]$ and possible units $[kN \cdot cm^2], [N \cdot mm^2]$ or $[N \cdot m^2]$. It can be seen that the bending stiffness depends on the type of material, expressed through the modulus of elasticity E, and on the shape (distribution of areas) of the cross-section, whose characteristics are determined by the axial moment of inertia I_x.

3. DIFFERENTIAL EQUATION OF THE ELASTIC CURVE OF A BENT BEAM

In a pure bending the elastic curve (in the deformed state) has the shape of a circular arc, as shown in Fig. 1b, where the radius of curvature is constant $R_k = const.$, because it depends only on the bending moment $M(z) = const.$, which is also constant in pure bending, see diagram of momentum in Fig. 1a. In the general case of bending by forces, if we neglect shear, the radius of curvature of the curve $y(z)$ that describes the shape of the elastic curve of the deformed beam depends on the bending moment, as given by Eq. (4). The slope of the tangent to the curve is the first derivative of the function $y(z)$: $y'(z) = tg\varphi$. Differentiating this expression with respect to z gives:

$$y''(z) = \frac{1}{cos^2\varphi} \frac{d\varphi}{dz} .$$

By applying the trigonometric relationship between the cosine and tangent functions, it follows that:

$$cos^2\varphi = \frac{1}{1+tg^2\varphi} = \frac{1}{1+\left(y'(z)\right)^2}.$$

Combining the last two expressions, we obtain:

$$\frac{d\varphi}{dz} = \frac{y''}{1+\left(y'(z)\right)^2}.$$

Since the element of the arc curvature is given by the Pythagorean theorem:

$$ds = \pm\sqrt{dz^2+dy^2} = \pm dz\sqrt{\left[1+\left(y'(z)\right)^2\right]},$$

thus:

$$dz = \frac{ds}{\pm\sqrt{\left[1+\left(y'(z)\right)^2\right]}}.$$

Since the curvature of elastic curve is $K = \frac{d\varphi}{ds} = \frac{1}{R_k}$, it follows that:

$$K = \frac{1}{R_k} = \frac{d\varphi}{ds} = \pm\frac{y''}{[1+(y')^2]^{\frac{3}{2}}}.$$

By applying the relationship between the radius of curvature of the elastic curve and the bending moment, as given in Eq. (4), we obtain:

$$K = \frac{1}{R_k} = \pm\frac{y''}{\sqrt{[1+(y')^2]^3}} = \frac{M(z)}{E\cdot I_x(z)}. \tag{5}$$

This is a nonlinear second-order differential equation, and its integral is elliptic. Elliptic integrals are solved graphically or numerically using computers and cannot be solved analytically. Timoshenko and Goodier (1952) [6] gave the same formula for calculating the elastic curves, *y*(*z*), of the supported beams of variable cross-section and loaded with bending moment *M*(*z*) in this nonlinear case.

The displacement of the centroid of the cross-section $z = z_C$ in the vertical direction $y(z)$ is called the deflection of the section f_C, as shown in Fig. 4. It also represents the ordinate of the elastic curve $f_C = y(z_C)$ measured relative to the z -axis. Since the length of the elastic curve in the neutral surface does not change, deflection causes a deviation of the centroid position relative to the vertical direction. As the deflections in beams within the elastic limit are very small compared to the length of the beam, this deviation is neglected. The deflection of the elastic curve is positive if the elastic curve moves downward relative to the initial position, and negative if it moves upward. Since the bending moment diagram is drawn so that it is positive on the lower side of the neutral line, when drawing the elastic curve, the y-axis is directed downward, making deflections positive together with bending moment, as in our physical reality.

In beam bending, not only does the centroid of the cross-section deflect, but the cross-section $z = z_C$ also rotates by an angle φ_C. This angle forms the tangent to the elastic curve $y'(z)$ of the bent beam relative to the initial position of the z -axis, so $tg\varphi$ is called the slope of the tangent to the elastic curve at the section at distance $z = z_C$, Fig. 4. For small angles: $y'(z) = tg\varphi \approx \varphi(z)$. The angle of the tangent slope to the elastic curve is positive

if its rotation relative to the initial position is clockwise. The units for the angle of rotation are radians or degrees.

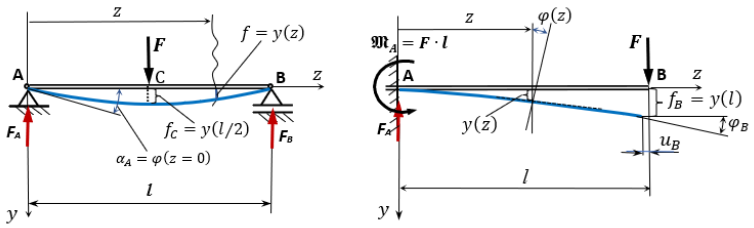

Fig. 4 The deflection of the section $f_C = y(z_C) = y(l/2)$ and the slope of the tangent to the elastic curve $y'(z) = \varphi(z)$ at distance z, $f_B = y(l)$ and φ_B the deflection and slope of the free end of cantilever beam [7].

In technical practice, for ideally elastic beams, deflections over total length of beam f/l greater than 2‰ are rare, which means $f/l < 1/500$. Because of this, the slopes of the sections are very small, so $\left(y'(z)\right)^2$ is a second-order small quantity relative to one ($\left(y'(z)\right)^2 \ll 1$, i.e., $1 + \left(y'(z)\right)^2 \approx 1$, so that $\left[1 + \left(y'(z)\right)^2\right]^{\frac{3}{2}} \approx 1$). Thus, Eq. (5) can be written in a simpler form:

$$\pm y'' = \frac{M(z)}{E \cdot I_x(z)} = \frac{M(z)}{\mathfrak{B}_x(z)}. \tag{6}$$

This is the approximate differential equation of the elastic curve. Therefore, the deflection of the elastic curve is the solution of this equation: $y(z) = f(z)$, and the slope is the first derivative of the elastic curve equation $y'(z) = \varphi(z)$.

In verifying the accuracy of the calculations, it was found, in our internal numerical calulstion and in [1], that the deviation of the deflection results obtained by the approximate differential Eq. (6) was up to 4% compared to the results obtained by the exact differential Eq. (5), and in extreme cases, the deviation was up to a maximum of 10%. With modern numerical methods, the elliptic integral can be solved, so if necessary, the exact solution of Eq. (5) can be determined. Approximate numerical methods, such as the finite element method (FEM) or finite difference method (FDM), are computationally efficient and can handle complex geometries and loading conditions more easily than exact solutions. Approximate solutions can be iteratively improved by refining the mesh or increasing the number of segments, thus approaching the exact solution.

Although numerical solutions for complex scenarios can be obtained, the basic understanding of the elastic curve concept is often missing when interpreting these solutions. In engineering practice, it is essential to grasp the solutions produced by software that employ approximate methods. Our approach seeks to link practical engineering solutions with the underlying significance of the results. To achieve this, a strong physical understanding of all the terms in mathematical models and their solutions is necessary.

It is necessary to determine which sign $(+)$ or $(-)$ is used in expression 6 to physically accept the solution. There are two cases, as explained in [7]:

1. When the bending moment is positive, $M(z) > 0$, the right side of expression (6) is positive, and the elastic curve has a maximum, so its second derivative is

negative, $y'' < 0$. In this case, the sign $(-)$ must be adopted so that the left side of the expression is also positive.

2. When the bending moment is negative, $M(z) < 0$, the right side of expression (6) is negative, and the elastic curve has a minimum, so its second derivative is positive, $y'' > 0$. In this case, the sign $(-)$ must be adopted in front of y'' so that the left side of expression (6) is negative.

From this, it follows that the approximate differential equation of the elastic curve of the beam in both cases is in the form:

$$y'' = -\frac{M(z)}{E \cdot I_x(z)} = -\frac{M(z)}{\mathfrak{B}(z)} = f(z),$$

thus,

$$\mathfrak{B}(z) \cdot y'' = -M(z). \tag{7}$$

The bending stiffness $\mathfrak{B}(z) = \mathfrak{B}_x(z) = E \cdot I_x(z)$ of the beam along the x-axis generally depends on the z-coordinate, as there are beams with variable bending stiffness.

For a prismatic beam with a constant cross-section, the moment of inertia I_x for the neutral x-axis is constant. Since the modulus of elasticity E is unchanged, it follows that the bending stiffness $\mathfrak{B} = E \cdot I_x = const$ is also constant. Only the bending moment $M(z)$ depends on the z-coordinate, which represents the distance from the left end of the beam.

The direct integration method is based on integrating the differential equation of the elastic curve of the beam, Eq. (7). Since $y'(z) = dy/dz$, we have

$$\mathfrak{B} \cdot y'(z)dy = -M(z)dz.$$

By integrating this equation in the first step, we obtain the slope of the elastic curve $y'(z)$:

$$\mathfrak{B} \cdot y'(z) = \int f(z)\, dz + C_1,$$

and by performing a second successive integration, we obtain the deflection of the elastic curve $y(z)$:

$$\mathfrak{B} \cdot y(z) = \int \Phi(z)\, dz + C_1 \cdot z + C_2 = \Psi(z) + C_1 \cdot z + C_2.$$

During these integrations, we introduce the integration constants C_1 and C_2, which are determined from the beam support conditions (boundary conditions, i.e. conditions for zero deflections and rotation angles in a specific type of support). The necessary condition that must be met is the continuity of the elastic curve, i.e. the first derivative must exist at every cross-section $y'(z)$: $y_1(a) = y_2(a)$ $y_1'(a) = y_2'(a)$, where $y_1(z), y_1'(z)$ for $0 \le z \le a$ and $y_2(z), y_2'(z)$ for $a \le z \le l$ are the laws of deflection and slope of the cross-section in the first and second interval directly before and after the section at a distance a.

For a beam with n segments, each segment correspont to different bending moment expression, there will be $2n$ integration constants. By integrating, a system of $2n$ linear equations is obtained for the corresponding integration constants. After determining these constants, analytical expressions for the slope $y_i'(z)$ and deflection $y_i(z)$ can be written for all segments of the beam.

4. CLEBSCH PROCEDURE

Alfred Clebsch's paper titled „Theorie der Elasticitat Fester Korper“ from 1862 and later Macaulay's paper titled "The Elastic Deflection of Beams" from 1919 provided closed-form equations for the deflection of beams subjected to various types of loading and support conditions. This allowed engineers to compute deflections directly and efficiently without extensive iterative calculations per segment. The Clebsch procedure (also known as Macaulay's procedure) for calculating beam deflections uses a double direct integration method in a piecewise procedure to assess the impact of loads on different beam segments. This approach simplifies the analysis of beams under complex loading conditions.

The purpose of this procedure is to write a single expression for the bending moment over the entire span of the beam, which is then solved using expression (7) to obtain unique integration constants and unique expressions for the slope and deflection of the elastic curve of the beam. To apply this procedure, the following steps need to be taken in order:

1. Determine the reactions at the supports;
2. Set the coordinate origin at the left end of the beam;

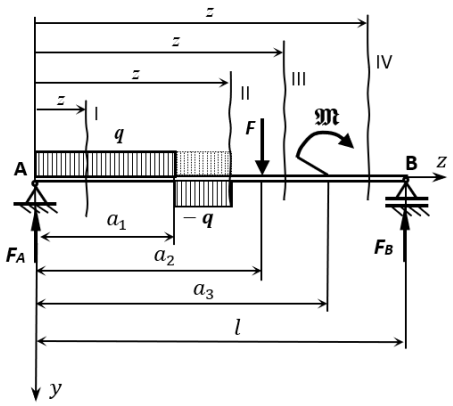

Fig. 5 Defined ranges I, II, III and IV according to the Clebsch procedure in general case of beam loading, [7].

3. Define the fields (intervals) in which certain (different) laws of change of the bending moment apply. In each part of the span (field) where the bending moment changes according to a certain law, the variable $(z - a_i)$ is taken, where a_i is the distance from the left boundary of that part of the span.
4. The bending moment in the next interval must be equal to the bending moment of the previous interval increased by a term containing the binomial $(z - a_i)$, which is achieved by extending the continuous load to the end of the beam while simultaneously subtracting the same amount of opposite load, as shown in Fig. 5.
5. The integration constants C_1 and C_2 are placed in the first field of the integral of the differential equation to apply to the entire span of the beam and are determined from the boundary conditions.
6. Each subsequent field is separated by a bold (Clebsch) line, and only the moments from the load in the corresponding field are added.

Applied to the case in Fig. 5, the expression for the bending moment of the beam has the form:

$$M_f = M(z) = F_A \cdot z - \frac{1}{2}q \cdot z^2\Big\| + \frac{1}{2}q(z-a_1)^2\Big\| - F(z-a_2)\| + \mathfrak{M}(z-a_3)^0$$

$$0 \le z \le a_1 \qquad a_1 \le z \le a_2 \qquad a_2 \le z \le a_3 \qquad a_3 \le z \le l$$

The second-order differential equation of the elastic curve Eq. (7) for the beam from Fig. 5 has the form:

$$\mathfrak{B} \cdot y'' = -F_A \cdot z + \tfrac{1}{2}q \cdot z^2\Big\| - \tfrac{1}{2}q(z-a_1)^2\Big\| + F(z-a_2)\| - \mathfrak{M}(z-a_3)^0.$$

After the first integration, we obtain the equation for the slope of the elastic curve, which includes an undetermined constant C_1:

$$\mathfrak{B} \cdot y' = -\tfrac{F_A}{2} \cdot z^2 + \tfrac{1}{6}q \cdot z^3 + C_1\Big\| - \tfrac{1}{6}q(z-a_1)^3\Big\| + \tfrac{F}{2}(z-a_2)^2\Big\| - \mathfrak{M}(z-a_3)^1. \quad (8)$$

After the next integration, we obtain the equation for the deflection of the beam elastic curve, which includes additional undetermined constant C_2:

$$\mathfrak{B}y = -\tfrac{F_A}{6}z^3 + \tfrac{1}{24}qz^4 + C_1 z + C_2\Big\| - \tfrac{1}{24}q(z-a_1)^4\Big\| + \tfrac{F}{6}(z-a_2)^3\Big\| - \tfrac{\mathfrak{M}}{2}(z-a_3)^2 \quad (9)$$

Since, the integration constants must have dimensions that match the other terms in the previous equations we can specify theirs physical interpretation. Specifically, C_1 has the dimension of force times length squared F L^2, same dimension as the flexural rigidity of the beam $\mathfrak{B}$. The constant C_2 has the dimension of force times length cubed F L^3. From the Eq. (8) we can conclud that the ratio $C_1/\mathfrak{B}$ determines the slop of the elastic curve at the left support when $z = 0$**.** Additionally, from Eq. (9), the ratio $C_2/\mathfrak{B}$ defines the deflection value at the left-hand side of the overhanging beam. This conclusion is illustrated in the following example of a loaded beam with overhangs.

The value of the constants are determined from the boundary conditions of the beam supports.

The fixed support A, for $z = 0$, of the beam given at Fig. 5, is without the deflection $y(z = 0) = 0$. From this condition, by substituting up to the first bold line in Eq. (9), we get $C_2 = 0$.

The movable support B, at $z = l$, has also a deflection equal to zero: $y(z = l) = 0$, so by substituting $z = l$ into the last equation, it follows that:

$$C_1 = \frac{F_A}{6} \cdot l^2 - \frac{1}{24}q \cdot l^3 + \frac{1}{24}q\left(1 - \frac{a_1}{l}\right)^4 + \frac{F}{6}\left(1 - \frac{a_2}{l}\right)^3 - \frac{\mathfrak{M}}{2}\left(1 - \frac{a_3}{l}\right)^2.$$

From the last expression, it is evident that the first integration constant depends not only on the value of the applied load (F, q and $\mathfrak{M}$) but also on its distribution and position a_i.

The integration constants C_1 and C_2 obtained in this way are substituted into the expressions for the deflection $y(z)$, Eq. (9), and the slope $y'(z)$, Eq. (8), of the elastic curve

of the beam for any z, thus providing analytical expressions for determining the deflection and slope at any cross-section along the span of the beam:

$$y(z) = \frac{1}{\mathfrak{B}}\left\{-\frac{F_A}{6}\cdot z^3 + \ \ldots\right\},$$
$$y'(z) = \frac{1}{\mathfrak{B}}\left\{-\frac{F_A}{2}\cdot z^2 + \cdots\right\}.$$

In the following section, several examples of beams with overhangs and different loading conditions are examined. Numerical experiments with varying loading distributions and values are connected to the interpretation of the integration constants.

5. NUMERICAL RESULTS AND DISCUSSION

Let us find the elastic curve equation for the beam shown in Fig. 6 by applying the Clebsch procedure described in the previous section. The reactions at the supports are $F_A = 3F/2 + 4\cdot q\cdot a$ and $F_B = 3F/2$. The unique bending moment expression for the beam length is:

$$M(z) = -\mathrm{F}\cdot z\| + F_A\cdot(z-a)\| - 2\mathrm{F}\cdot(z-3a) - \frac{1}{2}q\cdot(z-3\mathrm{a})^2\Big\| + F(z-4\mathrm{a})\| + F_B(z-5\mathrm{a})$$

The differential equation of elastic curve Eq. (7) for this beam is:

$$\mathfrak{B}\cdot y'' = \mathrm{F}\cdot z\| - F_A\cdot(z-a)\| + 2\mathrm{F}\cdot(z-3a) + \tfrac{1}{2}q\cdot(z-3\mathrm{a})^2\Big\| - F(z-4\mathrm{a})\| - -F_B(z-5\mathrm{a}).$$

After the first integration, it follows that:

$$\mathfrak{B}\cdot y'(z) = \frac{\mathrm{F}}{2}\cdot z^2 + C_1\Big\| - \frac{F_A}{2}\cdot(z-a)^2\Big\| + \mathrm{F}\cdot(z-3a)^2 + \frac{1}{6}q(z-3a)^3\Big\| - -\frac{\mathrm{F}}{2}(z-4\mathrm{a})^2\Big\| - \frac{F_B}{2}\cdot(z-5a)^2. \quad (10)$$

After the next integration, it follows that:

$$\mathfrak{B}\cdot y(z) = \frac{\mathrm{F}}{6}\cdot z^3 + C_1\cdot z + C_2\Big\| - \frac{F_A}{6}\cdot(z-a)^3\Big\| + \frac{\mathrm{F}}{3}\cdot(z-3a)^3 + \frac{1}{24}q(z-3a)^4\Big\| - -\frac{\mathrm{F}}{6}(z-4\mathrm{a})^3\Big\| - \frac{F_B}{6}\cdot(z-5a)^3. \quad (11)$$

The value of the constants are determined from the boundary conditions of the beam supports.

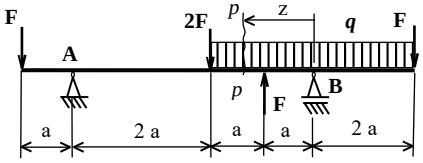

Fig. 6 Elastic beam with overhangs and discrete and continuoes loading

The fixed support A, for $z = a$, of the beam given at Fig. 6, is without the deflection $y(z = a) = 0$. From this condition, by substituting up to the first bold line in Eq. (11), we get:

$$C_1 \cdot a + C_2 = -\frac{\mathrm{F}}{6} \cdot a^3$$

The movable support B, at $z = 5a$, also has a deflection equal to zero: $y(z = 5a) = 0$, so by substituting $z = 5a$ into Eq. (11), the following equation stands:

$$5C_1 \cdot a + C_2 = -\frac{70\mathrm{F}}{3} \cdot a^3 + \frac{32\mathrm{F}_A}{3} \cdot a^3 - \frac{3q}{2}a^4.$$

By solving the system of two algebraic equations, we obtain the solution for the integration constants:

$$C_1 = (-139 \cdot F + 64 \cdot \mathrm{F}_A - 9 \cdot q \cdot a) \cdot \frac{a^2}{24} \tag{12}$$

$$C_2 = (135 \cdot F - 64 \cdot \mathrm{F}_A + 9 \cdot q \cdot a) \cdot \frac{a^3}{24} \tag{13}$$

Equations (10) and (11) are used for numerically drawing the elastic curve for the overhanging steel beam ($E = 2{,}1 \cdot 10^4 [kN/cm^2] = 2{,}1 \cdot 10^5 [MPa]$) shown in Fig. 7. The deflection value along the beam length, $y\,(z) = f[m]$, is calculated for a nonstandard I profile. Table 1 contains the values of the height h and the moment of inertia $I_x = h^4/12\,[1 - (1 - 2\psi)^3(1 - \psi)]$ of the nonstandard profile I with the thickness-to-width ratio $\psi = \delta/h = 0{,}2$ for different loading values. These loading values are the same as those used for the numerical calculation of deflection shown in Fig. 7.

We apply the criterion of the ultimate bending strength (flexural strength $\sigma_{df} = 10\,[kN/cm^2]$) of steel for dimensioning beams. According to this criterion, the bending stress must be less than the ultimate bending strength:

$$\sigma_z = \frac{M_{max}(z)}{W_x} \leq \sigma_{df} \tag{14}$$

where the elastic section modulus is $W_x[cm^3] = \frac{I_x}{h/2} = \frac{h^3}{6}[1 - (1 - 2\psi)^3(1 - \psi)]$. Thus, the expression for obtaining the dimension of height h becomes:

$$h[cm] \geq \sqrt[3]{\frac{6 \cdot M_{max}(z)}{\sigma_{df} \cdot [1 - (1 - 2\psi)^3(1 - \psi)]}} \tag{15}$$

Therefore, the characteristic dimension of the profile – the height h is determined according to the maximum value of the bending moment $M_{max}(z)$ for each type of beam, considering the values and distribution of the load.

In this context, the observed examples of overhanging beams have the same nonstandard I profile but different bending stiffnesses $\mathfrak{B} = E \cdot I_x$, as each is dimensioned individually according to the varying loading values and distribution that affect changes in the maximum value of the bending moment $M_{max}(z)$. In Table 1 one can find for $F = 1\,[kN]\ and\ q = 1\,[kN/m]$ calculated value of height $h = 6{,}62014\,[cm]$ and the moment of inertia $I_x = 132{,}403\,[cm^4]$. For $F = 3\,[kN]\ and\ q = 3\,[kN/m]$ it is height $h = 9.54789\,[cm]$ and the moment of inertia $I_x = 572.873\,[cm^4]$. From the coloured values in Table 1, we also observe the equality of certain values due to the symmetries of loading concentrated force and specific distribution of loading.

Table 1 The values of the height h and the moment of inertia I_x $[cm^4]$ of the profile I for the overhanging beam loading data used in calculation presented in Fig. 7

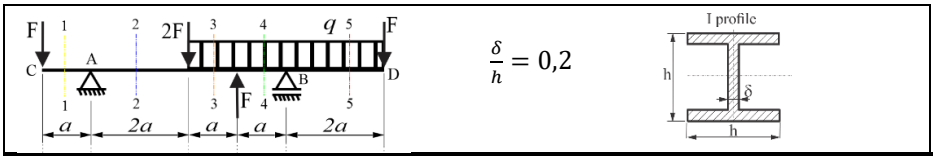

$a = 1\ [m]$,

$F\ [kN]$	$q = 1\ [kN/m]$		$q = 2\ [kN/m]$		$q = 3\ [kN/m]$	
	$h[cm]$	$I_x[cm^4]$	$h[cm]$	$I_x[cm^4]$	$h[cm]$	$I_x[cm^4]$
-3	6.62014	132.403	6.33193	110.809	6.01479	90.2219
-2	5.66014	70.7517	5.25441	52.5441	5.25441	52.5441
-1	4.17042	20.8521	5.25441	52.5441	6.62014	132.403
1	6.62014	132.403	7.57816	227.345	8.34085	333.634
2	7.57816	227.345	8.34085	333.634	8.98491	449.245
3	8.34085	333.634	8.98491	449.245	9.54789	572.873

Table 2 The values of the height h and the moment of inertia $I_x[cm^4]$ of the profile I for the overhanging beam loading data used in calculation presented in Table 3

$a = 1\ [m]$,

$F\ [kN]$	$q = 1\ [kN/m]$		$q = 2\ [kN/m]$		$q = 3\ [kN/m]$	
	$h[cm]$	$I_x[cm^4]$	$h[cm]$	$I_x[cm^4]$	$h[cm]$	$I_x[cm^4]$
-1	4.17042	20.8521	5.25441	52.5441	6.62014	132.403
-0.5	4.17042	20.8521	6.01479	90.2219	7.13133	178.283
-0.1	5.07307	45.6577	6.50791	123.65	7.49301	217.297
0.1	5.42402	59.6642	6.72868	141.302	7.66145	237.505
0.5	6.01479	90.2219	7.13133	178.283	7.97773	279.221
1	6.62014	132.403	7.57816	227.345	8.34085	333.634

The total length of the beam is $7 \cdot a$, where $a = 1\ [m]$. The different scenarios of loading combinations are illustrated in Fig. 7. From these diagrams, it can be observed that the deflection orientation is influenced by the direction of the concentrated force. Intuitively, the orientation of the deflection depends on the direction of the applied load. Since the value and sign of the integration constant C_2 determine the deflection value and orientation at the left-hand side of the overhanging beam, we conclude that this also depends on the directions of the applied loads.

For numerical signs of the forces and constant C_2, refer to Fig. 7. From expression (13), we observe that the sign of the constant C_2 depends not only on the sign and value of the force F, but also on the sign and value of the specific loading q, as well as the loading distribution defined by the value of a. Thus, the same beam with the same loads is further examined in terms of the varying signs of the constant C_2, which specifies the orientation of the deflection, as well as the so-called "dog's tail movement" of the beam's overhangs.

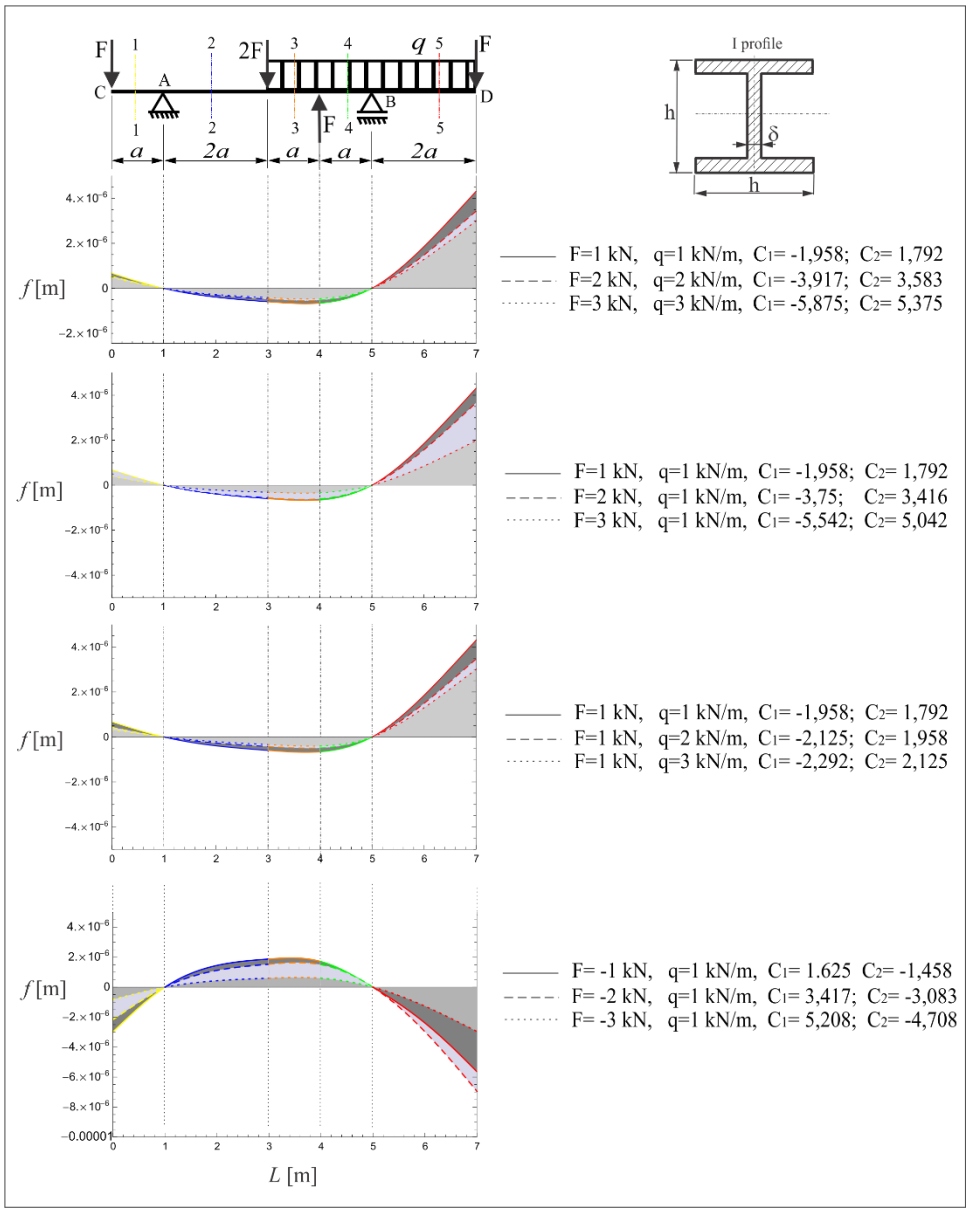

Fig. 7 The elastic curve represents the deflection values along the beam length $(y\,(z) = f[m])$ for different scenarios of loading values and combinations. The beam has a nonstandard I profile cross-section with $\delta/h = 0{,}2 \;\; and \;\; a = 1\;[m]$.

From the highlighted cells of Table 3, we conclude that for different values of $a\;[m]$ and specific loading $q\;[kN/m]$, the change in the sign of the constant $C_2\;[kNm^3]$ occurs regularly if the value of the force $F\;[kN]$ is between -0.5 and -0.1. Only for $q = 3\;[kN/m]$

and a=2 [m], this change occurs for $-1 < F\,[kN] < -0.5$. Therefore, the change in the sign of the constant C_2 does not occur only if the direction of the load changes; in these cases, the load remains in the same direction, but the orientation of the deflection changes.

Table 3 The values of the integration constants $C_1[kNm^2]$ and $C_2\ [kNm^3]$ for different values and distributions of loading on an overhanging beam with a nonstandard I profile cross-section.

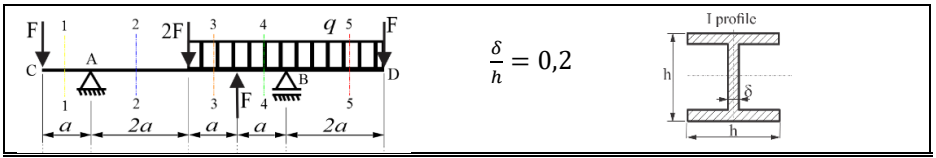

$q = 1\ [kN/m]$

$F\ [kN]$	$a = 1\ [m]$		$a = 1{,}5\ [m]$		$a = 2\ [m]$	
	$C_1[kNm^2]$	$C_2[kNm^3]$	$C_1[kNm^2]$	$C_2[kNm^3]$	$C_1[kNm^2]$	$C_2[kNm^3]$
-1	1.625	-1.45833	3.46875	-4.64063	5.83333	-10.333
$-0{,}5$	0.729167	-0.64583	1.45313	-1.89844	2.25	-3.8333
$-0{,}1$	0.0125	0.004167	-0.15938	0.295312	-0.61667	1.36667
0,1	-0.34583	0.329167	-0.96563	1.39219	-2.05	3.96667
0,5	-1.0625	0.979167	-2.57813	3.58594	-4.91667	9.16667
1	-1.95833	1.79167	-4.59375	6.32813	-8.5	15.6667

$q = 2\ [kN/m]$

$F\ [kN]$	$a = 1\ [m]$		$a = 1{,}5\ [m]$		$a = 2\ [m]$	
	$C_1[kNm^2]$	$C_2[kNm^3]$	$C_1[kNm^2]$	$C_2[kNm^3]$	$C_1[kNm^2]$	$C_2[kNm^3]$
-1	1.45833	-1.29167	2.90625	-3.79688	4.5	-7.6667
$-0{,}5$	0.5625	-0.47917	0.890625	-1.05469	0.916667	-1.1667
$-0{,}1$	-0.15417	0.170833	-0.72188	1.13906	-1.95	4.03333
0,1	-0.5125	0.495833	-1.52812	2.23594	-3.38333	6.63333
0,5	-1.22917	1.14583	-3.14063	4.42969	-6.25	11.8333
1	-2.125	1.95833	-5.15625	7.17188	-9.83333	18.3333

$q = 3\ [kN/m]$

$F\ [kN]$	$a = 1\ [m]$		$a = 1{,}5\ [m]$		$a = 2\ [m]$	
	$C_1[kNm^2]$	$C_2[kNm^3]$	$C_1[kNm^2]$	$C_2[kNm^3]$	$C_1[kNm^2]$	$C_2[kNm^3]$
-1	1.29167	-1.125	2.34375	-2.95313	3.16667	-5
$-0{,}5$	0.395833	-0.3125	0.328125	-0.21094	-0.41667	1.5
$-0{,}1$	-0.32083	0.3375	-1.28437	1.98281	-3.28333	6.7
0,1	-0.67917	0.6625	-2.09062	3.07969	-4.71667	9.3
0,5	-1.39583	1.3125	-3.70313	5.27344	-7.58333	14.5
1	-2.29167	2.125	-5.71875	8.01563	-11.1667	21

This indicates that there must be a specific value of the loads (in the observed case the value of concentrated force $F\ [kN]$), at which the sign of the deflection at the free end of the beam changes. From the shaded values in Table 4, we observe that the change deflection orientation is very sensitive to small changes in the value of the concentrated force. Therefore, a very small change in the value of the concentrated force, which does not change direction, but varies in the third or fourth decimal place, plays a key role in changing the direction of the deflection. Between these small differences in the value of

the concentrated force, there is also the phenomenon where the beam has no deflection at the free end. This phenomenon has been observed in engineering practice. It is very useful to know the load values at which the so-called "dog's tail movement" occurs at the overhangs of the beams.

Table 4 The sensitivity of sign changes of the integration constants $C_1[kNm^2]$ and $C_2\ [kNm^3]$ for different values of loading on an overhanging beam with a nonstandard I profile cross-section and total length 7 $[m]$

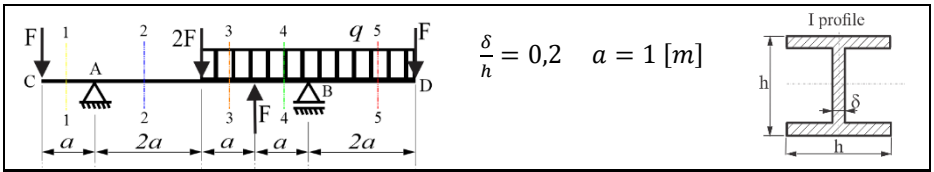

$F[kN]$	$q = 1\ [kN/m]$		$q = 2\ [kN/m]$		$q = 3\ [kN/m]$	
	$C_1[kNm^2]$	$C_2[kNm^3]$	$C_1[kNm^2]$	$C_2[kNm^3]$	$C_1[kNm^2]$	$C_2[kNm^3]$
−0,0930	-0.0000416	0.0155417	-0.166708	0.182208	-0.333375	0.348875
−0,0931	0.0001375	0.0153792	-0.166529	0.182046	-0.333196	0.348712
−0,102	0.0160833	0.000916667	-0.150583	0.167583	-0.31725	0.33425
−0,103	0.017875	-0.00070833	-0.148792	0.165958	-0.315458	0.332625
−0,186	0.166583	-0.135583	-0.0000833	0.0310833	-0.16675	0.19775
−0,187	0.168375	-0.137208	0.00170833	0.0294583	-0.164958	0.196125
−0,205	0.200625	-0.166458	0.0339583	0.00020833	-0.132708	0.166875
−0,206	0.202417	-0.168083	0.03575	-0.0014167	-0.130917	0.16525
−0,279	0.333208	-0.286708	0.166542	-0.120042	-0.000125	0.046625
−0,280	0.335	-0.288333	0.168333	-0.121667	0.0016667	0.045
−0,307	0.383375	-0.332208	0.216708	-0.165542	0.0500417	0.001125
−0,308	0.385167	-0.333833	0.2185	-0.167167	0.0518333	-0.0005

The next example of an overhanging beam we are analysing also has both concentrated and continuous transverse loads, differently distributed compared to the previous example. An additional impact on the change in deflection orientation and the values of the integration constants that characterize the deflection and slope at the left free end of the beam is caused by the axial force, which in this example is transferred to the beam through an eccentricity, Fig. 8. By applying the same Clebsch procedure and dimensioning using expression (15), it is straightforward to obtain the expressions for deflection and slope represents by the beam's elastic curve equation. We do not present the same procedure a second time; instead, we emphasize the numerical results that suggest variations in the orientation of the elastic curve, not only by changing the orientation of the loading but especially by increasing the value of the concentrated forces. From the second diagram, in Fig. 8, of the elastic curve for the value $F = 3\ [kN]$, we obtain $C_2 = 3.389[kNm^3]$, which has a positive value compared to the negative values of C_2 for $F = 1\ [kN]$ or $F = 2\ [kN]$ for the same $q = 1\ [kN/m]$. This trend of upward orientation of deflection continues for increased $F = 4\ [kN]$ or $F = 5\ [kN]$, as can be seen in the last diagram of Fig. 8. This change in deflection orientation due to the increase in force value is caused by the eccentric axial force, which significantly increases the local bending moment at the point where the eccentricity is attached. This directly affects the deflection values and thus

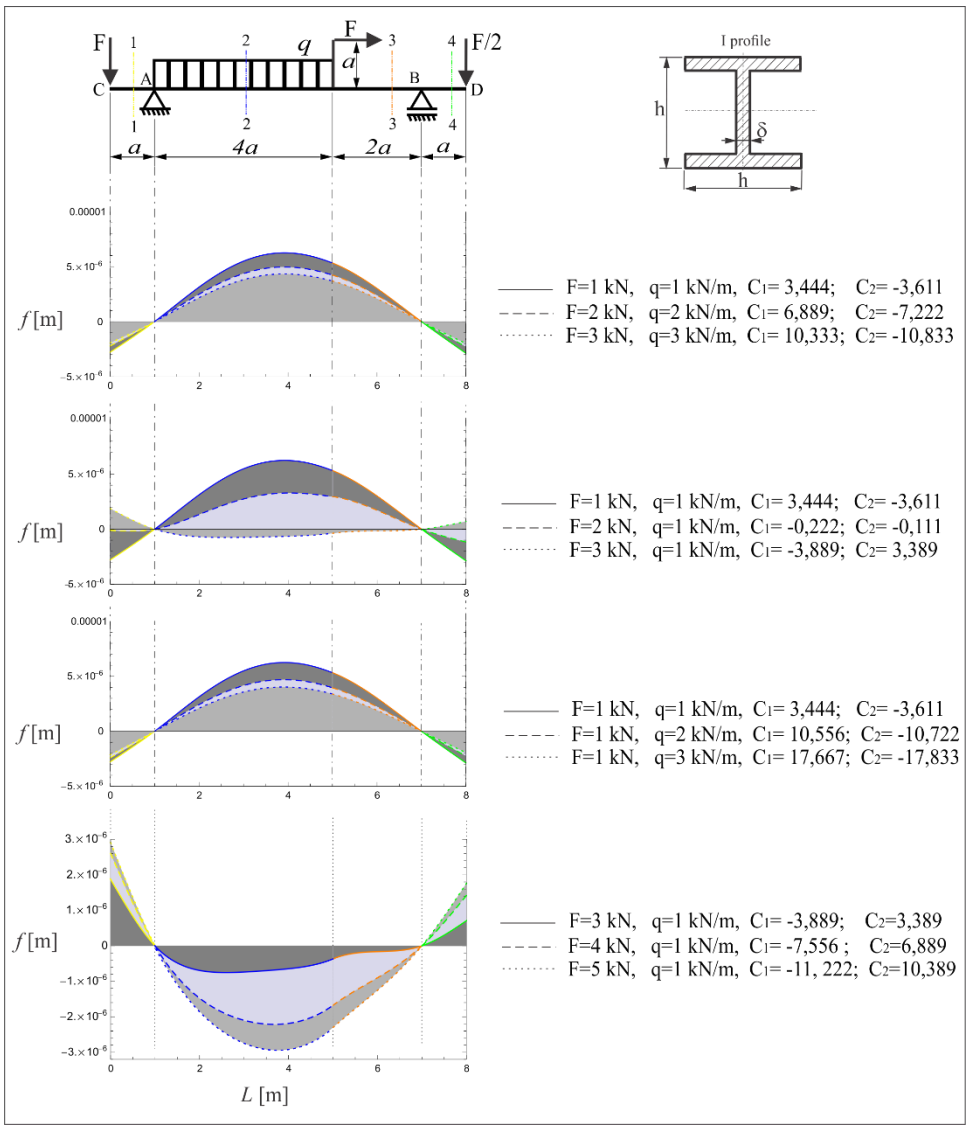

Fig. 8 The elastic curve $(y\ (z) = f[m])$ of an overhanging beam with an additional axial loading force for different scenarios of loading values and combinations. The beam has a nonstandard I profile cross-section with $\delta/h = 0{,}2\ \ and\ \ a = 1\ [m]$.

changes the scenario of the entire orientation of the elastic curve. This is even more evident in the values shown in Table 5, where the sign changes of the constant C_2 occur at increasingly higher force values with the increase in span a, as this directly increases the eccentricity and the local bending moment.

Table 5 The values of the integration constants $C_1[kNm^2]$ and $C_2\ [kNm^3]$ for different values and distributions of loading on an overhanging beam with additional eccentric axial loading of a nonstandard I profile cross-section.

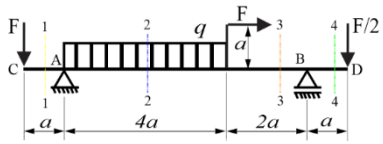

$\frac{\delta}{h} = 0{,}2$

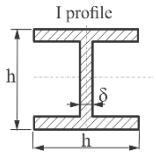

$q = 1\ [kN/m]$

$F[kN]$	$a = 1\ [m]$		$a = 1{,}5\ [m]$		$a = 2\ [m]$	
	$C_1[kNm^2]$	$C_2[kNm^3]$	$C_1[kNm^2]$	$C_2[kNm^3]$	$C_1[kNm^2]$	$C_2[kNm^3]$
1,5	1.6111111	−1.861111	11.625	−18.28125	34.888889	−71.77778
2,0	−0.222222	−0.111111	7.5	−12.375	27.555556	−57.77778
2,5	−2.055556	1.6388889	3.374999	−6.46875	20.22222	−43.77778
3,5	−5.722222	5.1388889	−4.875	5.34375	5.5555556	−15.77778
4,0	−7.555556	6.8888889	−9.00000	11.25	−1.777778	−1.777778
4,5	−9.388889	8.6388889	−13.125	17.15625	−9.111111	12.222222
5,5	−13.05556	12.138889	−21.375	28.96875	−23.77778	40.222222
6,0	−14.88889	13.888889	−25.5	34.875	−31.11111	54.222222
6,5	−16.72222	15.638889	−29.625	40.78125	−38.44444	68.222222

$q = 2\ [kN/m]$

$F[kN]$	$a = 1\ [m]$		$a = 1{,}5\ [m]$		$a = 2\ [m]$	
	$C_1[kNm^2]$	$C_2[kNm^3]$	$C_1[kNm^2]$	$C_2[kNm^3]$	$C_1[kNm^2]$	$C_2[kNm^3]$
1,5	8.7222222	−8.972222	35.625	−54.28125	91.77778	−185.5556
2,0	6.8888889	−7.222222	31.5	−48.375	84.44444	−171.5556
2,5	5.0555556	−5.472222	27.375	−42.46875	77.11111	−157.5556
3,5	1.3888889	−1.972222	19.12499	−30.65625	62.44444	−129.5556
4,0	−0.444444	−0.222222	15.0000	−24.75	55.11111	−115.5556
4,5	−2.277778	1.5277778	10.875	−18.84375	47.7778	−101.5556
5,5	−5.944444	5.0277778	2.625	−7.03125	33.11111	−73.55556
6,0	−7.777778	6.7777778	−1.5	−1.125	25.77778	−59.55556
6,5	−9.611111	8.5277778	−5.62500	4.78125	18.44444	−45.55556
7,5	−13.27778	12.027778	−13.875	16.59375	3.777778	−17.55556
8,5	−16.94444	15.527778	−22.125	28.40625	−10.88889	10.444444
9,5	−20.61111	19.027778	−30.375	40.21889	−25.55556	38.444444

$q = 3\ [kN/m]$

$F[kN]$	$a = 1\ [m]$		$a = 1{,}5\ [m]$		$a = 2\ [m]$	
	$C_1[kNm^2]$	$C_2[kNm^3]$	$C_1[kNm^2]$	$C_2[kNm^3]$	$C_1[kNm^2]$	$C_2[kNm^3]$
1,5	15.833333	−16.08333	59.625	−90.28125	148.6667	−299.3333
2,0	14.	−14.33333	55.5	−84.375	141.3333	−285.3333
2,5	12.166667	−12.58333	51.375	−78.46875	134.0000	−271.3333
3,5	8.4999999	−9.083333	43.12499	−66.65625	119.3333	−243.3333
4,0	6.6666667	−7.333333	39.00000	−60.75	112.0000	−229.3333
4,5	4.8333333	−5.583333	34.875	−54.84375	104.6667	−215.3333
5,5	1.166667	−2.083333	26.62499	−43.031249	89.9999	−187.3333
6,0	−0.666667	−0.333333	22.5	−37.125	82.6667	−173.3333
6,5	−2.500000	1.416667	18.375	−31.21875	75.3333	−159.3333
7,5	−6.166667	4.916667	10.125	−19.40625	60.6667	−131.3333
8,5	−9.83333	8.416667	1.874999	−7.5937499	45.9999	−103.3333
9,5	−13.50000	11.91667	−6.375	4.21875	31.3333	−75.3333

10,5	−17.16667	15.41667	−14.625	16.03125	16.6667	−47.3333
11,5	−20.83333	18.91667	−22.8750	27.84375	1.9999	−19.3333
12,5	−24.5	22.41667	−31.125	39.65625	−12.6667	8.6667

Table 6 The sensitivity of sign changes of the integration constants $C_1[kNm^2]$ and $C_2\ [kNm^3]$ for different values of loading on an overhanging beam with axial eccentricity, a nonstandard I profile cross-section and total length 6 $[m]$

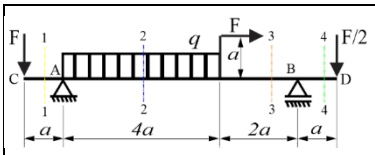

$\frac{\delta}{h} = 0{,}2 \quad a = 1\ [m]$

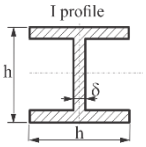

$F[kN]$	$q = 1\ [kN/m]$		$q = 2\ [kN/m]$		$q = 3\ [kN/m]$	
	$C_1[kNm^2]$	$C_2[kNm^3]$	$C_1[kNm^2]$	$C_2[kNm^3]$	$C_1[kNm^2]$	$C_2[kNm^3]$
1,0000	3.44444	-3.61111	10.5556	-10.7222	17.6667	-17.8333
1,9393	0.00034444	-0.323561	7.11146	-7.43467	14.2226	-14.5458
1,9394	-0.0000222	-0.323211	7.11109	-7.43432	14.2222	-14.5454
2,0000	-0.222222	-0.111111	6.88889	-7.22222	14.00000	-14.3333
2,0317	-0.338456	-0.0001611	6.77266	-7.11127	13.8838	-14.2224
2.0318	-0.338822	0.00018889	6.77229	-7.11092	13.8834	-14.222
3,0000	-3.88889	3.38889	3.22222	-3.72222	10.3333	-10.8333
3,8787	-7.11079	6.46434	0.00032222	-0.646772	7.11143	-7.75788
3,8788	-7.11116	6.46469	-0.0000444	-0.646422	7.11107	-7.75753
4,0000	7.55556	6.88889	-0.444444	-0.222222	6.66667	-7.33333
4,0634	-7.78802	7.11079	-0.676911	-0.0003222	6.4342	-7.11143
4,0635	-7.78839	7.11114	-0.677278	0.00002778	6.43383	-7.11108
5,0000	-11.2222	10.3889	-4.11111	3.27778	3.00000	-3.83333
5,8181	-14.2219	13.2522	-7.11081	6.14113	0.0003	-0.969983
5,8182	-14.2223	13.2526	-7.11118	6.14148	-0.000067	-0.969633
6,0000	-14.8889	13.8889	-7.77778	6.77778	-0.66667	-0.333333
6,0952	-15.238	14.2221	-8.12684	7.11098	-1.01573	-0.0001333
6,0953	-15.2383	14.2224	-8.12721	7.11133	-1.0161	0.00021667
7,0000	-18.5556	17.3889	-11.4444	10.2778	-4.33333	3.16667
10,000	-29.5556	27.8889	-22.4444	20.7778	-15.3333	13.6667

From the shaded values in Table 6, we observe that the change deflection orientation is very sensitive to small increases in the value of the force. Therefore, in this case of loading the overhanging beam with axial eccentricity, a very small increase of the value of the force plays a key role in changing the direction of the deflection. Between these small differences in the value of the force, there is also the phenomenon where the beam has no deflection at the free end. For example, when the force change value from $F = 4{,}0634\ [kN]$ to $F = 4{,}0635\ [kN]$, for $q = 2\ [kN/m]$, the negative value of the integration constant $C_2 = -0.0003222\ [kNm^3]$ goes to positiv value of $C_2 = 0.00002778\ [kNm^3]$. Between these two values (negative and positive), zero occurs, indicating the value and distribution of loading that keeps the overhang without deflection. The same situation occurs for different values of specific loading $q[kN/m]$, but within a different narrow range of force values, as indicated by the shaded cells in Table 6.

It is worth noting that the sensitivity of the free-end`s deflection and constants C_1 and C_2 to the concentrated force value in previous cases is logical since the position of the forces is on the overhangs.

The next case of the overhanging beam, presented in Fig. 9, with the same nonstandard I profile and cross-section characteristics, has both concentrated force and distributed loading on the overhangs. The third diagram of elastic curves in Fig. 9 shows that for same value of the force $F = 1\ [kN]$, deflection changes orientation between two close values of the specific loading $q = 1\ [kN/m]$ and $q = 2\ [kN/m]$. This indicates that in the observed case of distribution of loading, the values of the integration constants vary with respect to the specific loading $q\ [kN/m]$ values. From the shaded cells of Table 7, it is clear that with the increasing value of the concentrated force, the change in the sign of the integration constants occurs at higher values of specific loading for a shorter total length of the beam.

Table 7 The values of the integration constants $C_1[kNm^2]$ and $C_2\ [kNm^3]$ for different force $F[kN]$ and distributions of loading $q[kN/m]$ values on a beam with distributed loading on overhang of a nonstandard I profile cross-section.

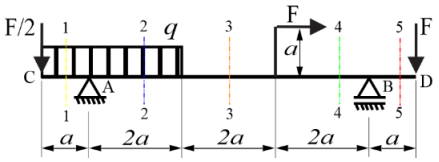

$\frac{\delta}{h} = 0{,}2$

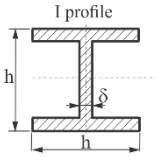

$F = 2\ [kN]$

$q[kN/m]$	$a = 1\ [m]$		$a = 1{,}5\ [m]$		$a = 2\ [m]$	
	$C_1[kNm^2]$	$C_2[kNm^3]$	$C_1[kNm^2]$	$C_2[kNm^3]$	$C_1[kNm^2]$	$C_2[kNm^3]$
1	−4.22222	4.013889	−7.6875	10.75781	−10.4444	18.88889
2	−2.61111	2.36111	−2.25	2.39063	2.44444	−7.55556
3	−1.00000	0.70833	3.1875	−5.97656	15.3333	−34.0000
4	0.61111	−0.94442	8.625	−14.3438	28.2222	−60.4444
5	2.22222	−2.59722	14.0625	−22.71094	41.1111	−86.8889
6	3.83333	−4.25	19.5	−31.07813	54.0000	−113.3333
7	5.44444	−5.90278	24.9375	−39.4453	66.8889	−139.7778
8	7.05556	−7.55556	30.375	−47.8125	79.7778	−166.2222
9	8.66667	−9.20833	35.8125	−56.17968	92.6667	−192.6667
10	10.2778	−10.8611	41.25	−64.54687	105.5556	−219.1111
11	11.8889	−12.5139	46.6875	−72.91406	118.4444	−245.5556

$F = 4\ [kN]$

$q[kN/m]$	$a = 1\ [m]$		$a = 1{,}5\ [m]$		$a = 2\ [m]$	
	$C_1[kNm^2]$	$C_2[kNm^3]$	$C_1[kNm^2]$	$C_2[kNm^3]$	$C_1[kNm^2]$	$C_2[kNm^3]$
1	−10.0556	9.68056	−20.8125	29.8828	−33.7778	64.2222
2	−8.4444	8.02778	−15.375	21.5156	−20.8889	37.7778
3	−6.8333	6.375	−9.9375	13.1484	−8.0000	11.3333
4	−5.2222	4.7222	−4.5	4.78125	4.88889	−15.1111
5	−3.6111	3.0694	0.9375	−3.58594	17.7778	−41.5556
6	−2.0000	1.41667	6.375	−11.9531	30.6667	−68.000
7	−0.38889	−0.23611	11.8125	−20.3203	43.5556	94.4444
8	1.22222	−1.88889	17.25	−28.6875	56.4444	−120.8889

9	2.8333	−3.54167	22.6875	−37.0547	69.3333	−147.3333
10	4.44444	−5.19444	28.125	−45.4219	82.2222	−173.7778
11	6.05556	−6.84722	33.5625	−53.7891	95.1111	−200.2222

$F = 6\ [kN]$

$q[kN/m]$	$a = 1\ [m]$		$a = 1{,}5\ [m]$		$a = 2\ [m]$	
	$C_1[kNm^2]$	$C_2[kNm^3]$	$C_1[kNm^2]$	$C_2[kNm^3]$	$C_1[kNm^2]$	$C_2[kNm^3]$
1	−15.8889	15.3472	−33.9375	49.0078	−57.1111	109.556
2	−14.2778	13.6944	−28.5	40.6406	−44.2222	83.1111
3	−12.6667	12.0417	−23.0625	32.2734	−31.3333	56.6667
4	−11.0556	10.3889	−17.625	23.9063	−18.4444	30.2222
5	−9.4444	8.73611	−12.1875	15.5391	−5.5556	3.7778
6	−7.8333	7.08333	−6.75	7.17187	7.3333	−22.6667
7	−6.2222	5.43056	−1.3125	−1.19531	20.2222	−49.1111
8	−4.6111	3.77778	4.125	−9.5625	33.1111	−75.5556
9	−3.0000	2.125	9.5625	−17.9296	46.0000	−102.0000
10	−1.38889	0.47222	15.0000	−26.2968	58.8889	−128.444
11	0.2222	−1.18056	20.4375	−34.6641	71.7778	−154.889

Table 8 The sensitivity of sign changes of the integration constants $C_1[kNm^2]$ and $C_2\ [kNm^3]$, for different values of specific distribution of loading on a beam with axial eccentricity, a nonstandard I profile cross-section and total length 8 $[m]$

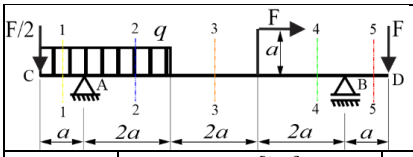

$\frac{\delta}{h} = 0{,}2 \quad a = 1\ [m]$

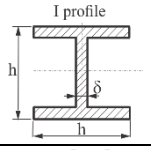

$q[kN/m]$	$F = 1\ [kN]$		$F = 2\ [kN]$		$F = 3\ [kN]$	
	$C_1[kNm^2]$	$C_2[kNm^3]$	$C_1[kNm^2]$	$C_2[kNm^3]$	$C_1[kNm^2]$	$C_2[kNm^3]$
1,0000	−1.305556	1.180556	−4.22222	4.013889	−7.13889	6.847222
1.8103	−0.0000722	−0.1586902	−2.9167389	2.674643056	−5.83340556	5.507976389
1.8104	0.0000889	−0.1588556	−2.9165778	2.674477778	−5.83324445	5.5078111
2,0000	0.30555556	−0.472222	−2.6111111	2.361111111	−5.5277778	5.1944445
3,0000	1.9166667	−2.125	−1.000000	0.708333333	−3.9166667	3.5416667
3,6206	2.9165222	−3.1507138	−0.0001444	−0.31738056	−2.9168111	2.51595278
3.6207	2.91668333	−3.1508791	0.00001667	−0.31754583	−2.9166500	2.5157875
4,0000	3.5277778	−3.777778	0.611111	−0.444444	−2.3055556	1.8888889
5,0000	5.138889	−5.4305555	2.222222	−2.59722222	−0.6944444	0.23611111
5,4310	5.83327778	−6.1429027	2.9166111	−3.30956944	−0.0000556	−0.476236
5,4311	5.83343889	−6.1430680	2.9167722	−3.30973472	0.0001056	−0.4764013
6,0000	6.750000	−7.083333	3.8333333	−4.2500000	0.9166667	−1.4166667

The observed trend of sensitivity in sign changes of the constants at higher values of specific loading $q[kN/m]$ with increasing force values is noticeable in Table 6 as well.

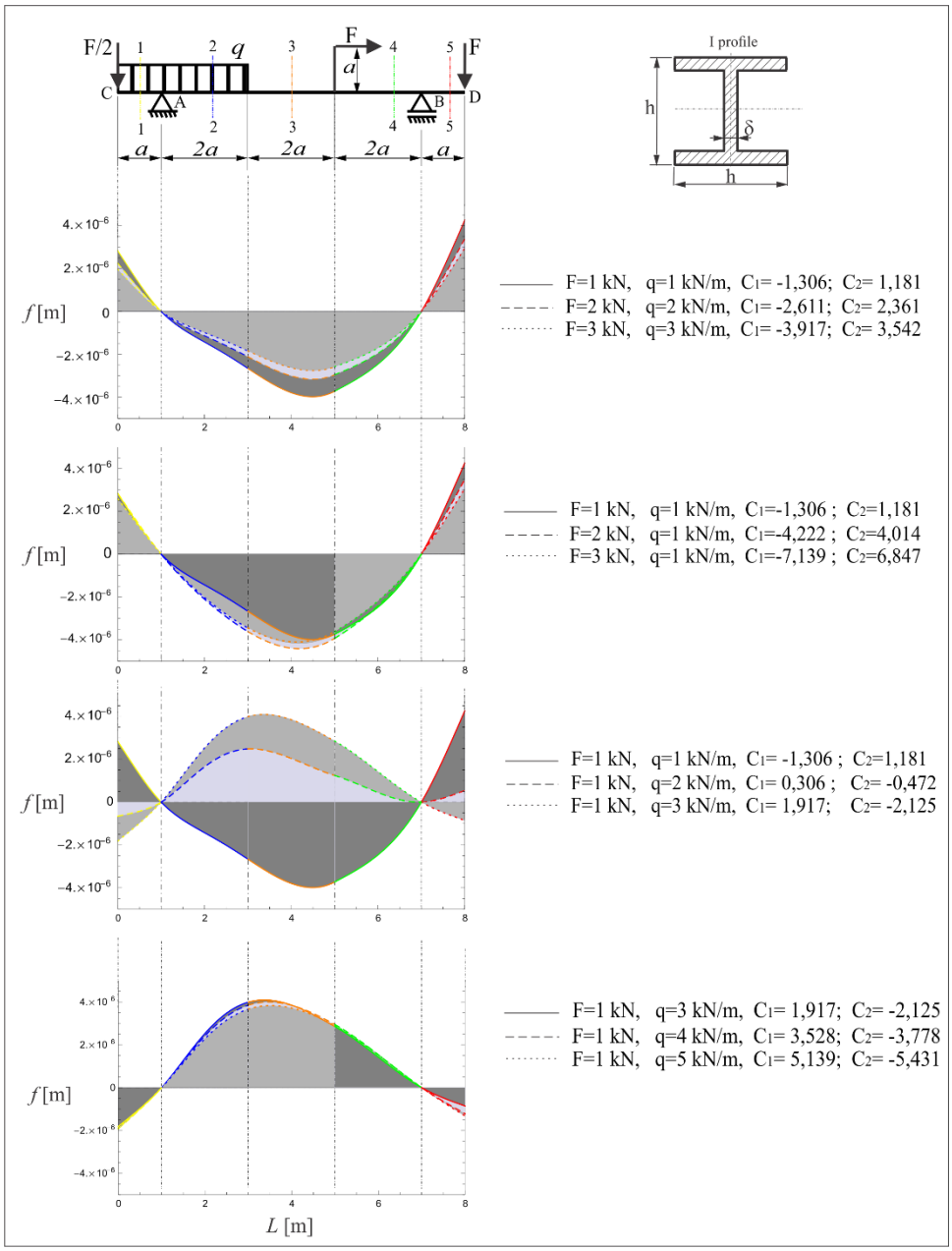

Fig. 9 The elastic curve ($y\,(z) = f[m]$) of a beam with axial eccentricity and distributed loading on the overhang for different scenarios of loading values and combinations. The beam has a nonstandard I profile cross-section with $\delta/h = 0{,}2$ and $a = 1\,[m]$.

6. CONCLUSION

In this study, we investigated the significance of integration constants for beam bending within the framework of linear elastic theory. We conducted a numerical analysis by employing the Clebsch procedure to explore various loading scenarios on overhanging beams. Our findings revealed that the values of integration constants fluctuated significantly in response to changes in loading conditions, indicating a direct relationship between the applied forces and the beam's deflection behaviour.

We found that as the application of point loads and distributed loads varied, the resulting deflection patterns showed high sensitivity to both the magnitude and direction of the applied forces. Specifically, an increase in concentrated force F led to a transition of the integration constants $C_1[kNm^2]$ and C_2 $[kNm^3]$ from negative to positive at certain load distributions, indicating a shift in deflection orientation. Moreover, we established that even minor alterations in the magnitude of the concentrated forces could lead to considerable changes in deflection behaviour. This phenomenon, known as "dog's tail movement", was particularly evident at the free-ends of overhanging beams, demonstrating the critical importance of accurately determining load factors in practical applications.

Additionally, the study highlighted the correlation between integration constants and bending stiffness. The bending stiffness denoted as $\mathbf{B}$ depends on the modulus of elasticity E and the moment of inertia I_x of the beam's cross-section. The ultimate bending strength of steel is used to determine dimensions of the beams, ensuring that the bending stress remains below this strength. The height of the beam is determined based on the maximum bending moment for each type of beam, considering the load values and distribution. Overhanging beams with the same nonstandard I profile but different height and bending stiffnesses are individually dimensioned according to the varying loads and their effects on the maximum bending moment. The bending stiffness varies because the height is determined individually for each example, which influences the deflection of the beam. On the other hand, the values of the integration constants depend only on the position of beam supports and the type and distribution of the load, while the dimensions of the cross-section of the beam do not affect them. The variability in the values and signs of these constants is highly sensitive to small changes in load values and significantly affects the overall shape of the elastic line of the bent beam. The combined influence of bending stiffness and integration constants significantly determines the shape of the deflected beam.

Our numerical results were consistent with theoretical predictions, affirming the relevance of integration constants. The observed deviations fell within acceptable ranges, which validated the effectiveness of combining the Clebsch method with modern numerical techniques. Overall, these findings underscore the essential role of integration constants in understanding beam deformation, pointing to the necessity for further research into varied loading conditions to fully appreciate their implications in engineering design and applications.

In future research, we plan to focus on a comparative analysis of the maximum deflections of beams for different load cases and their correlation with the values of the integration constants. So far, we have not considered this analysis because the maximum deflections depend on the shape of the beam's cross-section, and we have used the same shape, only changing the dimensions. In the next study, we will attempt to correlate these values and aim for the optimal selection of the cross-sectional shape that guarantees smaller deflections.

Acknowledgement: *This research was financially supported by the Ministry of Science, Technological Development and Innovation of the Republic of Serbia (Contract No. 451-03-136/2025-03/200109).*

REFERENCES

1. Bíró, I., Cveticanin, L., & Szuchy, P. (2018). Numerical method to determine the elastic curve of simply supported beams of variable cross section. *Structural Engineering and Mechanics*, 68(6), 713-720. DOI: https://doi.org/10.12989/sem.2018.68.6.713.
2. Shabana A.A., (2018) Computational Continuum Mechanics, Copyright © 2018 John Wiley & Sons, Ltd., p.368, ISBN:9781119293217.
3. Rojas, A.L. (2014), "A mathematical model of elastic curve for simply supported beams subjected to uniformly distributed load taking into account the shear deformations", *Int*. J. Innovat. *Comput*. Informat. *Contr*., 5(3), 885-890.
4. Rojas, A.L. and Espino, J.V.R. (2015), "Fixed-end moments for beams subjected to a concentrated forced localized anywhere taking into account the shear deformations", *Int*. J. Innovat. Comput. Informat. *Contr*., 11(2), 463-474.
5. Yavari, A., Sarkani, S. & Reddy, J. (2001). Generalized solutions of beams with jump discontinuities on elastic foundations. Archive of Applied Mechanics 71, 625–639 https://doi.org/10.1007/s004190100169.
6. Timoshenko, S. and Goodier, J.N. (1952), *Theory of Elasticity*, McGraw-Hill.
7. Јовановић Д. Б. и Симоновић Ј. (2023), Отпорност материјала машинских конструкција, универзитетски уџбеник, Машински факултет Универзитета у Нишу, Ниш: Графика Галеб, стр.332, ISBN 978-86-6055-168-1.